Cell Cycle–Regulated Attachment of the Ubiquitin-Related Protein SUMO to the Yeast Septins

Erica S. Johnson and Günter Blobel

Laboratory of Cell Biology, Howard Hughes Medical Institute, Rockefeller University, New York, New York 10021

Abstract. SUMO is a ubiquitin-related protein that functions as a posttranslational modification on other proteins. SUMO conjugation is essential for viability in *Saccharomyces cerevisiae* and is required for entry into mitosis. We have found that SUMO is attached to the septins Cdc3, Cdc11, and Shs1/Sep7 specifically during mitosis, with conjugates appearing shortly before anaphase onset and disappearing abruptly at cytokinesis. Septins are components of a belt of 10-nm filaments encircling the yeast bud neck. Intriguingly, only septins on the mother cell side of the bud neck are sumoylated. We have identified four major SUMO attachment-site lysine residues in Cdc3, one in Cdc11, and two in Shs1, all within the consensus sequence (IVL)KX(ED). Mutating these sites eliminated the vast majority of bud neck-associated SUMO, as well as the bulk of total SUMO conjugates in G_2/M-arrested cells, indicating that sumoylated septins are the most abundant SUMO conjugates at this point in the cell cycle. This mutant has a striking defect in disassembly of septin rings, resulting in accumulation of septin rings marking previous division sites. Thus, SUMO conjugation plays a role in regulating septin ring dynamics during the cell cycle.

Key words: Smt3 • SUMO • septin • cytoskeleton • protein processing

POSTTRANSLATIONAL modifications of proteins play critical roles in most cellular processes through their unique ability to cause rapid alterations in the functions of preexisting proteins, multiprotein complexes, and subcellular structures. One recently discovered modification involves the covalent attachment of the small ubiquitin-related protein SUMO to other proteins. SUMO, also known as sentrin or Ubl1 (Okura et al., 1996; Shen et al., 1996), or in yeast as Smt3[1] (Johnson et al., 1997), was originally discovered attached to the Ran GTPase-activating protein, RanGAP1[2] (Matunis et al., 1996; Mahajan et al., 1997), and has subsequently been shown to be conjugated to a rapidly growing set of substrates including IκBα, the inflammatory response regulatory protein (Desterro et al., 1998), and PML, a protein whose fusion to the retinoic acid receptor causes acute promyelocytic leukemia (Sternsdorf et al., 1997; Kamitani et al., 1998b; Müller et al., 1998). *Saccharomyces cerevisiae* cells deficient in SUMO conjugation are inviable and arrest in the cell cycle before anaphase (Seufert et al., 1995; Li and Hochstrasser, 1999). Thus, SUMO conjugation is a key regulatory mechanism in the growth control pathways of both yeast and higher eukaryotes.

SUMO is 18% identical to ubiquitin (Ub), a highly conserved 76-residue protein whose primary function is to target proteins for proteolysis, either by the 26S proteasome or by endocytosis into the lysosome or yeast vacuole (reviewed by Hershko and Ciechanover, 1998). All known functions of Ub involve its covalent attachment to other proteins, usually via an isopeptide bond between Ub's COOH-terminal carboxyl group and the ϵ-amino group of an internal Lys residue in the substrate. Proteins to be degraded by the proteasome are linked to a multi-Ub chain, in which successive copies of Ub are attached to an internal Lys residue of the previous Ub in the chain. Ub conjugation is carried out in three enzymatic steps, catalyzed by a Ub-activating enzyme (E1), one of a family of Ub-conjugating enzymes (E2s), and a Ub-protein ligase or recognin (E3). Ub conjugation can also be reversed by a family of deubiquitinating enzymes (Dubs) which cleave the isopeptide bond.

The SUMO and Ub conjugation pathways are entirely distinct, but share multiple similarities. In the first step of

Address correspondence to Dr. Erica S. Johnson, Department of Biochemistry and Molecular Pharmacology, Thomas Jefferson University, 233 South 10th Street, Philadelphia, PA 19107. Tel.: (215) 503-4616. Fax: (215) 503-5393. E-mail: Erica.Johnson@mail.tju.edu

1. We are calling the product of the *Saccharomyces cerevisiae SMT3* gene SUMO to bring the yeast terminology for this modification in line with the mammalian terminology.

2. *Abbreviations used in this paper:* GFP, green fluorescence protein; HA, influenza virus hemagglutinin epitope tag; MALDI-TOF, matrix-assisted laser desorption/ionization time of flight; NTA, nitriloacetic acid; RanGAP1, Ran GTPase-activating protein; ts, temperature sensitive; Ub, ubiquitin.

the SUMO conjugation pathway, SUMO is activated by a heterodimeric activating enzyme (E1) consisting of Aos1 and Uba2, proteins with sequence similarity to the NH_2 and COOH terminus, respectively, of Ub activating enzymes (Johnson et al., 1997; Okuma et al., 1999). The second enzyme in the SUMO pathway is Ubc9, a protein with strong sequence similarity to Ub-conjugating enzymes (E2s; Desterro et al., 1997; Gong et al., 1997; Johnson and Blobel, 1997; Schwarz et al., 1998). There are also specific proteases that cleave SUMO–substrate isopeptide bonds, one of which is encoded by the yeast *ULP1* gene (Li and Hochstrasser, 1999).

The function of SUMO conjugation is only beginning to be understood. There are four well-characterized substrates of mammalian SUMO: RanGAP1, IκBα, and two components of so-called PML nuclear bodies, PML and Sp100. In the cases of RanGAP1, Sp100, and PML, SUMO conjugation functions by altering the subcellular localization of its substrates. Attachment of SUMO targets the otherwise cytosolic RanGAP1 to the nuclear pore complex by promoting binding to Nup358/RanBP2 (Matunis et al., 1996; Mahajan et al., 1997), which is also sumoylated (Saitoh et al., 1998), whereas SUMO conjugation to PML and Sp100 is involved in their tight localization to the PML nuclear bodies (Sternsdorf et al., 1997; Müller et al., 1998). SUMO has an entirely different effect on IκBα, where it becomes attached to the major ubiquitination site, preventing ubiquitination and thereby protecting sumoylated IκBα from proteasome-dependent proteolysis (Desterro et al., 1998). As SUMO is only distantly related to Ub, it is very unlikely that SUMO itself targets proteins for proteasome-dependent proteolysis.

In *S. cerevisiae*, SUMO is encoded by the *SMT3* gene, which was originally isolated as a high-copy suppressor of mutations in *MIF2*, which encodes a centromere binding protein (Meluh and Koshland, 1995). SUMO conjugation is essential for yeast viability, as *SMT3*, *UBA2*, *AOS1*, *UBC9*, and *ULP1* are all essential genes (Dohmen et al., 1995; Seufert et al., 1995; Johnson et al., 1997; Li and Hochstrasser, 1999). The pattern of SUMO conjugates changes during the cell cycle (Li and Hochstrasser, 1999), and conditional mutants in the SUMO conjugation pathway arrest in the cell cycle after DNA replication, but before anaphase, with a short spindle and an undivided nucleus positioned on the mother cell side of the bud neck (Seufert et al., 1995; Li and Hochstrasser, 1999).

The yeast bud neck is a dynamic structure that is the focus of many processes involved in the polarized growth and division of yeast cells. Its primary structural feature is a belt of 10-nm filaments whose central components are members of a family of GTP-binding coiled-coil proteins called septins (reviewed by Longtine et al., 1996). Yeast contain seven septin genes, of which two are expressed only during sporulation, and five, *CDC3*, *CDC10*, *CDC11*, *CDC12*, and *SHS1/SEP7*, are expressed during vegetative growth. A septin-containing ring initially forms in the mother cell during G_1, ~15 min before bud emergence. After the bud appears, the ring extends into the bud, forming a continuous hourglass-shaped structure that appears as a "double ring." During cytokinesis, the 10-nm filaments visible by electron microscopy disappear, but the septin ring, as visualized by immunofluorescence microscopy, splits in half, and the remaining septin-containing structures are disassembled during the following G_1 phase.

The septin ring acts as a scaffold for the binding of other proteins (DeMarini et al., 1997). Proteins associated with the septins include those involved in chitin deposition (DeMarini et al., 1997), bud site selection (Chant et al., 1995; Sanders and Herskowitz, 1996), mating projection formation (Giot and Konopka, 1997), cytokinesis (Bi et al., 1998; Lippincott and Li, 1998a,b), and a checkpoint that monitors the presence of a septin ring before nuclear division (Carroll et al., 1998; Longtine et al., 1998; Barral et al., 1999). Septin mutations affect all of these functions. *CDC3* and *CDC12* are strictly essential genes, whereas *cdc10* and *cdc11* deletion strains are viable, but show severe defects in septin-related processes, especially at high temperatures. Mutants in *SHS1* display more subtle defects (Carroll et al., 1998; Mino et al., 1998). In conditional septin mutants at the nonpermissive temperature, all septins fail to localize to the bud neck, and cells develop multiple, branched, highly elongated buds, become multinucleate, and do not undergo cytokinesis.

As a first step toward understanding the physiological role of the SUMO conjugation pathway in *S. cerevisiae*, we were interested in identifying and characterizing substrate proteins that become modified by SUMO. We discovered that SUMO is attached to septins in a cell cycle-dependent manner and have investigated the functional consequences of impairing septin sumoylation.

Materials and Methods

Media and Genetic Techniques

Standard techniques were used (Ausubel et al., 1994). Rich yeast media, containing either 2% glucose (YPD) or 2% galactose (YPG), and synthetic yeast media were prepared as described (Sherman et al., 1986). Strains were cured of *URA3*-containing plasmids using 5-fluoroorotic acid (PCR Inc.; Boeke et al., 1984). Cell cycle arrests were induced by incubating for 3 h with 10 μM α-factor, 0.1 M hydroxyurea, or 15 μg/ml nocodazole (Sigma Chemical Co.).

Plasmid Constructions

The pRS315-derived (Sikorski and Hieter, 1989) plasmid p315-P_{GAL}-HFSMT3, for expressing His6- and FLAG-tagged SUMO(G98) from P_{GAL10}, has been described (Johnson et al., 1997). p315-CDC3-HA was pRS315-derived and contained ~1,000 bp of the 5′ flanking sequence of *CDC3* and the *CDC3* coding region fused to a COOH-terminal influenza virus hemagglutinin epitope tag (HA) sequence encoding GYPYDVPDYAAFL (Johnson et al., 1992). p315-CDC3-Δ94-HA lacked the coding region for the NH_2-terminal 94 residues of Cdc3, so that the expressed protein began MSQING. p315-P_{GAL}-CDC3-HA expressed full-length Cdc3-HA from P_{GAL10}. Plasmids expressing variants of Cdc3 with TEV protease cleavage sites or Lys to Arg mutations were produced by oligonucleotide-directed site-specific mutagenesis of p315-CDC3-HA using the Mutagene kit (BioRad) according to the manufacturer's instructions. Single stranded p315-CDC3-HA was produced using helper phage R408 (Promega Corp.). Partial protein sequences encoded by TEV site-containing Cdc3 constructs, including the altered segment are as follow: pCDC3-TEV-K2, RQH^{21}ENLYFQGSD^{26}VQI; pCDC3-TEV-K3, DGV^{39}ENLYFQGSQ^{48}NDD; pCDC3-TEV-K4, GLG^{69}ENLYFQGSQ^{76}SEK; pCDC3-TEV-K6, IRRQ^{95}ENLYFQGSI^{96}NGY. Introduced sequence is underlined. Superscripts indicate positions of amino acid residues in the unaltered sequence. TEV protease cleaves between Gln and Gly in the introduced sequence. Correctly mutagenized plasmids were identified by digesting with BamHI, whose cleavage site encodes the Gly-Ser in the introduced sequence. Plasmids containing Lys to Arg mutations in *CDC3* were identified by cleaving with the following restriction enzymes: K4R, PstI;

K11R, BamHI; K30R, AatII; K63R, BsiWI; K415R, BamHI; K443R, MscI. All oligonucleotide sequences and construction details are available on request.

Yeast Strains

S. cerevisiae strains used are listed in Table I. Strains in which the genomic copies of genes bear epitope tags, deletions, Lys to Arg mutations, or previously isolated mutant alleles, were produced by transforming yeast with the products of assembly PCR reactions, made as follows, which were integrated into the chromosome by homologous recombination. Three PCR products that overlapped by 17–20-bp were used as the templates in a second round PCR reaction using outside primers to produce a product containing the 5′ flanking sequence and/or the coding sequence of the gene of interest, with or without a tag or a mutation, followed by a selective marker and then the 3′ flanking sequence. Transformants were selected for the appropriate selective marker and were screened further by immunoblotting with an mAb against the HA epitope, by amplifying the gene of interest from chromosomal DNA and digesting with an appropriate restriction enzyme diagnostic for a point mutation, or by screening for the desired temperature sensitive (ts) phenotype. Strains containing multiple altered genes were derived from the single mutants by mating and tetrad dissection. Chromosomal DNA derived from MY254 (a generous gift of M. Yuste and F. Cross, Rockefeller University, NY, NY) and STX339-1C (Yeast Genetic Stock Center) was used as source of the *cdc15-2* and *cdc12-1* alleles, respectively. In constructing EJY309, the *SHS1* coding sequence was amplified in two overlapping pieces, one containing the K426R mutation and the other containing the K437R mutation with a BstBI restriction site included in the overlapping region between the two mutations. Cdc12 with a COOH-terminal green fluorescent protein (GFP) tag was constructed by inserting the *CDC12* coding sequence into pYX242-GFP (Rosenblum et al., 1998). As the high level of Cdc12-GFP expression produced from this plasmid was toxic to EJY318, but not to wild-type cells, we integrated the GFP tag into one of the *CDC12* loci in the diploids EJY318 and JD51, as described above, to produce EJY320 and EJY319, respectively. Cultures of EJY320 contained a greater proportion of abnormal cells than either the parental strain EJY318 or the wild-type control strain EJY319. All construction details and oligonucleotide sequences are available on request.

Antibodies

A rabbit polyclonal antibody was raised against NH_2 terminally His_6-tagged SUMO(G98) (Cocalico Biologicals) and was affinity purified on a His_6-FLAG-SUMO(G98) affinity column (Johnson et al., 1997) as described (Harlow and Lane, 1988). In a whole cell lysate from an arrested *ubc9* mutant, the affinity-purified anti-SUMO antibody recognized only free unconjugated SUMO (data not shown), demonstrating its specificity. A rabbit polyclonal antibody against Cdc3, a generous gift of J. Pringle (University of North Carolina, Chapel Hill, NC), was affinity purified on a nitrocellulose filter containing Cdc3-lacZ (expressed from pUR-PH1 [Kim et al., 1991] a gift of J. Pringle) as described (Pringle et al., 1991). The unpurified anti-Cdc3 serum recognized primarily an ~100-kD band unrelated to Cdc3. The affinity-purified antibody also contained a small amount of antibody against this other protein. Other antibodies used were the 16B12 mAb against the HA epitope (in Figs. 1 b, 3, 4 b, 5 b, and 6; Berkeley Antibody Co.), the 3F10 mAb against the HA epitope (in Fig. 2 a; Boehringer Mannheim Corp.), the B5-1-2 mAb against tubulin (a generous gift of Mike Rout, Rockefeller University, NY, NY), and a rabbit polyclonal antibody against Cdc11 (Santa Cruz Biotechnology).

Immunoblot Analyses of Whole Yeast Lysates and Immunoprecipitates

Yeast whole cell lysates were prepared as described (Yaffe and Schatz, 1984). Acetone-washed TCA precipitates were resuspended in 0.5 M Tris

Table I. S. cerevisiae Strains

Name	Relevant genotype	Source
DF5	*MAT***a**/*MATα trp1-1/trp1-1 ura3-52/ura3-52 his3-Δ200/his3-Δ200 leu2-3,112/leu2-3,112 lys2-801/lys2-801*	Finley et al., 1987
YWO102*‡	*MATα ubc9Δ::TRP1 leu2::ubc9Pro-Ser::LEU2*	Seufert et al., 1995
EJY251-11b*	*MATα smt3Δ::HIS3*	Johnson et al., 1997
EJY300*	*MAT***a** *cdc3Δ::HIS3*	This study
JD51	*MAT***a**/*MATα trp1-Δ1/trp1-Δ1 ura3-52/ura3-52 his3-Δ200/his3-Δ200 leu2-3,112/leu2-3,112 lys2-801/lys2-801*	Dohmen et al., 1995
JD52§	*MAT***a**	J. Dohmen (Heinrich-Heine-Universität, Düsseldorf, Germany)
EJY301§	*MAT***a** *CDC3-HA::HIS3*	This study
EJY302§	*MAT***a** *CDC10-HA::HIS3*	This study
EJY303§	*MAT***a** *CDC11-HA::HIS3*	This study
EJY304§	*MAT***a** *CDC12-HA::HIS3*	This study
EJY305§	*MAT***a** *SHS1-HA::HIS3*	This study
EJY306§	*MAT***a**/*MATα CDC3-HA::HIS3/CDC-HA::HIS3*	This study
EJY307§	*MAT***a** *cdc3-Δ94-HA::TRP1*	This study
EJY308§	*MAT***a** *cdc11-R412-HA::HIS3*	This study
EJY309§	*MAT***a** *shs1-R426,437-HA::HIS3*	This study
EJY310§	*MAT***a** *cdc3-Δ94-HA::TRP1 cdc11-R412-HA::HIS3*	This study
EJY311§	*MAT***a** *cdc3-Δ94-HA::TRP1 cdc11-R412-HA::HIS3 shs1-R426,437-HA::HIS3*	This study
EJY312§	*MAT***a** *cdc3-R4,11,30,63-HA::TRP1*	This study
EJY316§	*MAT***a** *cdc3-R4,11,30,63-HA::TRP1 cdc11-R412-HA::HIS3 shs1-R426,437-HA::HIS3*	This study
EJY318§	*MAT***a**/*MATα cdc3-R4,11,30,63-HA::TRP1/cdc3-R4,11,30,63-HA::TRP1 cdc11-R412-HA::HIS3/cdc11-R412-HA::HIS3 shs1-R426,437-HA::HIS3/shs1-R426,437-HA::HIS3*	This study
EJY319§	*MAT***a**/*MATα CDC12-GFP::URA3/CDC12*	This study
EJY320§	*MAT***a**/*MATα cdc3-R4,11,30,63-HA::TRP1/cdc3-R4,11,30,63-HA::TRP1 cdc11-R412-HA::HIS3/cdc11-R412-HA::HIS3 shs1-R426,437-HA::HIS3/shs1-R426,437-HA::HIS3 CDC12-GFP::URA3/CDC12*	This study
EJY321§	*MAT***a** *cdc15-2::URA3*	This study
EJY322§	*MAT***a** *CDC3-HA::HIS3 cdc15-2::URA3*	This study
EJY323§	*MAT***a** *cdc3-R4,11,30,63-HA::TRP1 cdc12-1::TRP1*	This study

*Derived from DF5.
‡Our isolate appears to be disomic for Chr III including the *leu2::ubc9Pro-Ser::LEU2* allele.
§Derived from JD51.

base, 6.5% SDS, 100 mM dithiothreitol (DTT), and 12% glycerol, heated at 65°C for 20 min and the debris removed by microcentrifugation. Lysates were subjected to immunoblotting, followed by chemiluminescent detection as described (Johnson et al., 1997). For anti–HA-epitope immunoprecipitations, 45 μl of lysate (~1 mg protein) was added to 1.5 ml RIPA buffer (50 mM Tris, pH 7.5, 150 mM NaCl, 5 mM EDTA, 1% Triton X-100) containing 2 μg/ml of each of the protease inhibitors antipain, aprotinin, chymostatin, leupeptin, and pepstatin, plus 50 mM N-ethylmaleimide (Sigma Chemical Co.). 10 μl of anti-HA–Sepharose (Berkeley Antibody Co.) was added, followed by incubation at 4°C for 2 h with rotation. Beads were washed three times with RIPA buffer plus 0.1% SDS, resuspended in Laemmli loading buffer lacking reducing agent, and incubated at 65°C for 20 min. The supernatant was removed, supplemented to 100 mM DTT, and analyzed by SDS-PAGE and immunoblotting as described.

For the TEV protease cleavage experiment, washed HA–Sepharose beads bearing Cdc3-HA variants were washed once with 50 mM Tris, pH 8.0, 0.5 mM EDTA, and 1% Triton X-100, and incubated with 20 U TEV protease (Life Technologies) for 4 h at 25°C in 20 μl of the same buffer. HA-Sepharose beads were pelleted by centrifugation, and the supernatant "unbound" fraction was removed. One 20 μl wash of the beads with RIPA buffer and 0.1% SDS was added to the unbound fraction, and the beads were washed three times with 1 ml RIPA buffer and 0.1% SDS and prepared for SDS-PAGE as described above to yield the "bound" fraction.

Isolation of SUMO-conjugated Proteins

EJY251-11b containing p315-P_{GAL}-HFSMT3 was grown at 30°C in 4 liter of YP containing 2% raffinose and 1% galactose to an A_{600} of 2. Cells were harvested by centrifugation and lysed 10 min on ice in 200 ml cold 1.85 NaOH, 7.5% β-mercaptoethanol. Protein was precipitated by addition of 200 ml 50% TCA, collected by centrifugation, and the pellet was washed with 200 ml ice-cold acetone. The pellet was resuspended in 400 ml Buffer A (6 M guanidine HCl, 100 mM sodium phosphate, 10 mM Tris/HCl, pH 8.0) and incubated at 25°C for 1 h with rotating. Lysates were clarified by centrifugation at 27,000 g_{max}, adjusted to pH ~7.0 (measured using pH paper) with 1 M Tris base, supplemented to 20 mM imidazole, and bound in batch for 2 h to 2 ml of Ni-nitriloacetic acid (NTA) agarose (Qiagen). The Ni-NTA agarose was loaded into a column, washed with 20 ml of Buffer A, and then with 100 ml of Buffer B (8 M urea, 100 mM sodium phosphate, 10 mM Tris, pH 6.3), and then eluted with 200 mM imidazole in Buffer B. 4 ml of the eluate was added to 46 ml RIPA buffer containing 0.1% SDS, 1 mM PMSF, and 1 mM β-mercaptoethanol, and bound in batch overnight at 4°C to 0.4 ml anti-FLAG sepharose (IBI/Kodak). The anti-FLAG Sepharose was loaded into a column, washed with 50 ml of RIPA buffer with 0.1% SDS, and then eluted with 100 mM glycine, pH 2.2, 150 mM NaCl, 1% Triton X-100, and 0.1% SDS. The eluate was fractionated on a 5–20% acrylamide gel. Protein bands detected by staining with Coomassie brilliant blue were excised and identified by direct analysis of a Lys-C endoproteinase digest by matrix-assisted laser desorption/ionization time of flight (MALDI-TOF) mass spectrometry at the Rockefeller University Protein/DNA Technology Center (NY, NY) as described (Gharahdaghi et al., 1996). Two different bands yielded fragments of 1032.6, 1226.6, 1274.8, 1356.2, 1607.9, 1844.6, 1995.86, 2268.5, and 3574.5 D, which match the masses predicted by a theoretical digest of Cdc3. Some of the other bands identified contained other sumoylated proteins, but many contained proteins that bound nonspecifically to the affinity columns.

Fluorescence Microscopy

Yeast cells were prepared for indirect immunofluorescence microscopy essentially as described (Pringle et al., 1991). Cells were fixed in 3.7% formaldehyde for 10 min. Proteins were visualized by incubating with the primary antibodies described above, followed by Cy3-conjugated donkey anti–rabbit IgG or fluorescein (DTAF)-conjugated donkey anti–mouse IgG (Jackson Laboratories). Cells were mounted in 4′,6-diamidino-2-phenylindole (DAPI)-containing medium to visualize DNA. GFP fluorescence and Calcofluor staining of bud scars were visualized in live yeast stained with Fluorescent Brightener 28 (Calcofluor white; Sigma Chemical Co.) as described (Pringle, 1991). All micrographs were taken using a 63× oil objective on a Axiophot microscope (Carl Zeiss). Images were transferred directly to Adobe Photoshop 3.05 using a Sony DKC-5000 digital photo camera. Overlaying of Cy3 and fluorescein signals in double-label immunofluorescence microscopy experiments was done in Adobe Photoshop.

Results

Septins Are Modified by SUMO during Mitosis

To identify substrates of the SUMO pathway, we constructed a strain that expressed His6- and FLAG-tagged SUMO as its only copy of the SUMO-encoding *SMT3* gene. When proteins bearing both tags were purified by affinity chromatography, the resulting fraction contained a smear of high molecular weight bands (Fig. 1 a), similar to the previously observed pattern of SUMO conjugates in yeast (Johnson et al., 1997; Li and Hochstrasser, 1999). Two of these bands were identified by direct mass spectrometric analysis of a protease digestion mixture (see Materials and Methods) as containing the product of the *S. cerevisiae CDC3* gene.

To confirm that Cdc3 could be modified by SUMO and to ask whether any of the other four yeast septins expressed during vegetative growth were sumoylated, we tagged the genomic copies of the *CDC3*, *CDC10*, *CDC11*, *CDC12*, and *SHS1* genes with the HA epitope tag (Field et al., 1988). The HA-tagged versions of all five septins were functional and were incorporated normally into the septin ring at the bud neck (not shown). When these strains were treated with nocodazole (see below), significant amounts of higher molecular weight forms of Cdc3, Cdc11, and Shs1 were observed, whereas Cdc10 and Cdc12 were present only as single species of the predicted molecular weight (Fig. 1 b, lanes 1–5). Immunoprecipitation of the HA-tagged septins and immunoblotting with a polyclonal antibody against SUMO confirmed that all of the high molecular weight species of Cdc3, Cdc11, and Shs1 contained SUMO (Fig. 1 b, lanes 6–10).

To test whether septin sumoylation is cell cycle depen-

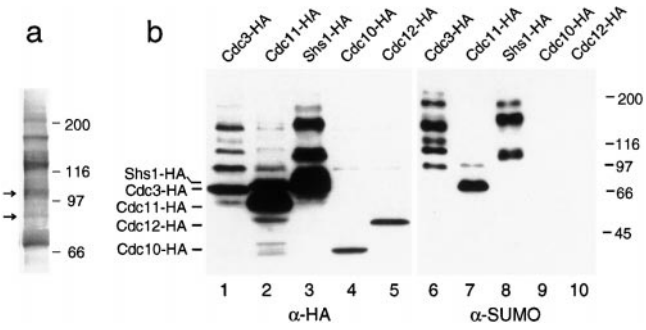

Figure 1. SUMO is attached to the septins Cdc3, Cdc11, and Shs1. a, Lysate from cells expressing His_6- and FLAG epitope-tagged SUMO was subjected to affinity chromatography on Ni-NTA agarose and anti-FLAG agarose. The resulting fraction was analyzed by SDS-PAGE and Coomassie brilliant blue staining. Bands determined to contain Cdc3 by MALDI-TOF mass spectrometry are indicated by arrows. b, Whole cell lysates (lanes 1–5) or anti-HA immunoprecipitates (lanes 6–10) from nocodazole-arrested cells expressing HA-tagged septins were analyzed by SDS-PAGE and immunoblotting with an mAb against the HA epitope (lanes 1–5) or with a polyclonal antibody against SUMO (lanes 6–10). Lanes 1 and 6, EJY301; lanes 2 and 7, EJY303; lanes 3 and 8, EJY305; lanes 4 and 9, EJY302; lanes 5 and 10, EJY304. The HA-tagged septin in each lane is indicated. Bands corresponding to unmodified HA-tagged septins are indicated.

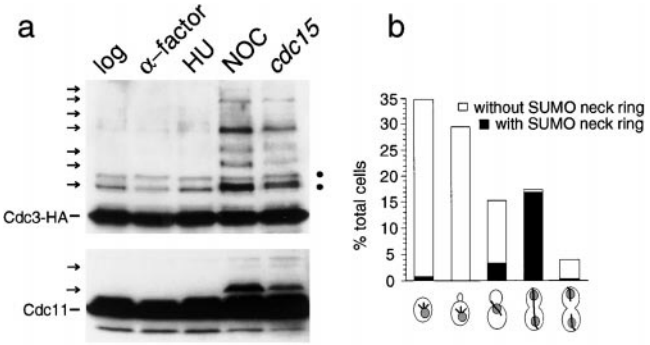

Figure 2. Cell-cycle dependent attachment of SUMO to the septins. a, Whole cell lysates from EJY301 (*CDC3-HA*), growing exponentially (log) or arrested with α-factor, hydroxyurea (HU), or nocodazole (NOC), or from EJY322 (*CDC3-HA cdc15-2*) that had been arrested at 37°C for 3 h (*cdc15*), were analyzed by SDS-PAGE and immunoblotting with an mAb against the HA epitope (top) or a polyclonal antibody against Cdc11 (bottom). Bands corresponding to unmodified Cdc3-HA and to Cdc11 are indicated. Arrows indicate the positions of SUMO-modified species. Circles indicate bands that cross-react with the anti-HA antibody. b, Exponentially growing wild-type (DF5) cells were analyzed by double-label immunofluorescence microscopy with a polyclonal antibody against SUMO and an mAb against tubulin. Height of bars represents the percentage of total cells in each of the five categories illustrated below the histogram: unbudded cells, small-budded cells (buds less than one third the size of the mother cell), large-budded cells with a short spindle, cells undergoing nuclear division with an intact elongated spindle, and cells with a divided nucleus and broken spindle. Black bars represent the portion containing a SUMO ring at the bud neck. 424 total cells were counted.

dent, cells expressing Cdc3-HA were arrested in G_1 with the mating pheromone α-factor, in the S phase checkpoint with hydroxyurea, in the G_2/M spindle checkpoint with nocodazole, or in late anaphase with the ts *cdc15-2* allele. In all cases, >90% of cells were arrested at the appropriate point in the cell cycle (data not shown). Both Cdc3-HA and Cdc11 were most heavily modified in nocodazole-arrested cells and somewhat less so in *cdc15*-arrested cells (Fig. 2 a). Very little, if any, of either septin was modified in α-factor- or hydroxyurea-arrested cells, although the results were partially obscured by cross-reacting bands.

To define the stages when septins are sumoylated in more detail, SUMO was visualized by double label immunofluorescence microscopy. The protein detected in addition to SUMO was either Cdc3-HA (Fig. 3) or tubulin (Fig. 2 b), whose localization was used to determine the stage of the cell cycle occupied by individual cells. SUMO localized to the nucleus at all points in the cell cycle (Fig. 3, a, e, j, and o; data not shown), but more strikingly it localized to a ring at the bud neck only during mitosis. Specifically, a ring of SUMO appeared at the bud neck of large budded cells just before initiation of anaphase spindle elongation and nuclear division (Figs. 2 b and 3 e). This SUMO ring persisted through anaphase (Figs. 2 b and 3 j) and it disappeared abruptly at cytokinesis, virtually simultaneously with septin ring separation (Fig. 3, o and p) and the beginning of spindle breakdown (Fig. 2 b). Surprisingly, the SUMO ring did not completely colocalize with the septins. SUMO coincided only with the mother cell side of the septin "double ring," appearing on the side next to the undivided nucleus or on the side of the larger cell in mitotic cells (Fig. 3, e, i, j, and n). Thus, SUMO conjugation to the septins was asymmetrical with respect to the mother–bud axis.

Identification of the SUMO Attachment Sites in Cdc3

To determine the function of septin sumoylation, we wanted to generate yeast mutants in which septins would not be modified. The most direct way to eliminate septin sumoylation specifically was to identify the Lys residues that serve as SUMO attachment sites and to replace them with Arg residues, which cannot be modified, thereby eliminating septin sumoylation without disturbing conjugation to other substrates.

Our initial approach to identifying SUMO attachment sites on Cdc3 was to affinity-purify SUMO-Cdc3 conjugates from strains expressing Cdc3-HA and His6- and FLAG-tagged SUMO(G98) or SUMO(A98). These preparations varied only in the identity of the COOH-terminal residue of SUMO, which is the residue involved in the isopeptide bond with the substrate. This material was digested with trypsin and with endoproteinase Lys C and analyzed by MALDI-TOF mass spectrometry with the goal of identifying species varying by the 14 mass unit difference between the COOH-terminal Gly and Ala in the two preparations. One such species was identified, with a molecular weight of 2,327 D, which was consistent with SUMO attachment at Lys11 of Cdc3 (data not shown).

Examination of the sequence surrounding Lys11 revealed that three other Lys residues in the NH_2-terminal domain of Cdc3 were embedded in similar sequence motifs having the consensus (IVL)KXE, which appeared to be a potential sumoylation site consensus sequence. Since there are multiple SUMO-Cdc3 conjugate bands (Fig. 1), such a consensus sequence might be used in either of two different ways. SUMO might be attached at one or the other of these Lys residues as a chain containing SUMO–SUMO linkages, analogous to the multi-Ub chain. Alternatively, multiple single copies of SUMO might be attached with one SUMO moiety per Lys residue. To distinguish between these possibilities, we designed a series of constructs containing cleavage sites for the TEV protease at different sites along the NH_2-terminal domain of Cdc3, either after the first two Lys residues (TEV-K2), after the third (TEV-K3), after the fourth (TEV-K4), or after the sixth (TEV-K6; see Fig. 4 a). These constructs also contained a COOH-terminal HA tag, which was used to immunoprecipitate the Cdc3 variants from lysates of nocodazole-arrested yeast. Immunoprecipitated proteins were cleaved with TEV protease while still bound to the beads and separated into an unbound fraction containing the fragment NH_2-terminal to the cleavage site, and a bound fraction containing the COOH-terminal cleavage product. This experiment showed that for each additional Lys residue included NH_2-terminal to the TEV site, an additional sumoylated species appeared on the NH_2-terminal product and disappeared from the COOH-terminal product. There was one major NH_2-terminal SUMO-containing

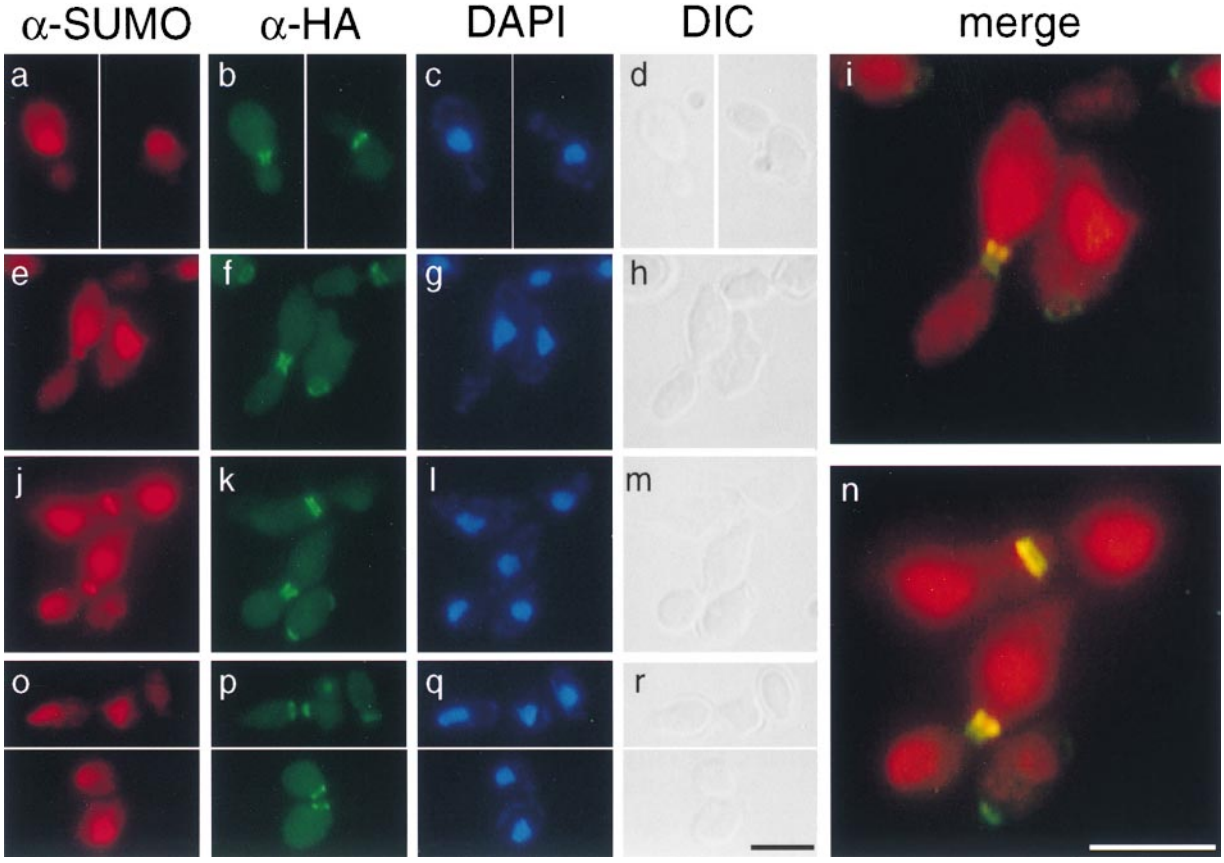

Figure 3. SUMO localizes to the mother cell side of the septin ring during mitosis. Double-label immunofluorescence microscopy of EJY306 (*CDC3-HA/CDC3-HA*) using a polyclonal antibody against SUMO (red; a, e, j, and o) and an mAb against the HA epitope (green; b, f, k, and p). Cells were visualized by differential interference contrast (DIC; d, h, m, and r) and DNA by DAPI staining (c, g, l, and q). Panels i and n are overlays of the anti-SUMO and anti-HA signals in the fields shown in e–h and j–m, respectively. Colocalization is represented by yellow in the overlays. Bars, 5 μm.

species from TEV-K2, two from TEV-K3, and three from TEV-K4 and TEV-K6 (Fig. 4 e), and there were two major SUMO-containing COOH-terminal cleavage products from TEV-K2, one from TEV-K3, and none from TEV-K4 or TEV-K6 (Fig. 4 d, cleavage products are indicated; lanes 2, 3, and 5 contained uncleaved species, see Fig. 4 b). These results were generally consistent with a model where single copies of SUMO are attached to Cdc3 at three to four major sites, at Lys-4 and/or Lys-11, at Lys-30, and at Lys-63. A separate experiment in which these Lys residues were altered by site-directed mutagenesis showed that both Lys-4 and Lys-11 can serve as sumoylation sites (data not shown).

However, this model does not completely explain the pattern of high molecular weight SUMO conjugates on Cdc3, which consisted of seven bands between ~95 and ~200 kD (Fig. 4 c, lanes 1–5). For several reasons, it is more likely that the additional bands reflect the presence of another mobility-altering factor, rather than attachment of multiple copies of SUMO at the same Lys residue. One is that cleavage at the TEV-K2 site produced only two detectable SUMO-containing COOH-terminal fragments (Fig. 4 d, lane 2). This result can be explained most easily if a single mobility-altering factor lies NH_2-terminal to the TEV site at position 27. Once the NH_2 terminus is cleaved off, the number of bands associated with the COOH-terminal fragment would reflect the number of attached SUMO moieties, whereas NH_2-terminal fragments would still be present in two forms for every SUMO moiety. This explanation is also consistent with the pattern of NH_2-terminal cleavage products, where there is a minor band above each of the three major SUMO-containing bands from TEV-K4 and TEV-K6 (Fig. 4 e, lanes 4 and 5). A second reason is that several of the SUMO-Cdc3 bands and corresponding NH_2-terminal TEV cleavage product bands appear to be too close together to differ by a whole SUMO moiety. Free SUMO runs at ~20 kD on SDS-PAGE, but two of the pairs of SUMO-Cdc3 bands appeared to differ by significantly less than 20 kD, and the first two sets of major and minor NH_2-terminal cleavage products appeared to differ by 10 kD or less (Fig. 4 c, lane 1, and e, lanes 4 and 5). A third reason is that the TEV-K4 variant significantly reduced the amount of the third SUMO-containing conjugate with a proportionate increase in the second band, but there was no reduction in intensity or change in position of the fourth or sixth SUMO-containing bands (Fig. 4 c, lane 4, cf lanes 1–3, and 5). This result is most easily explained if the TEV-K4 mu-

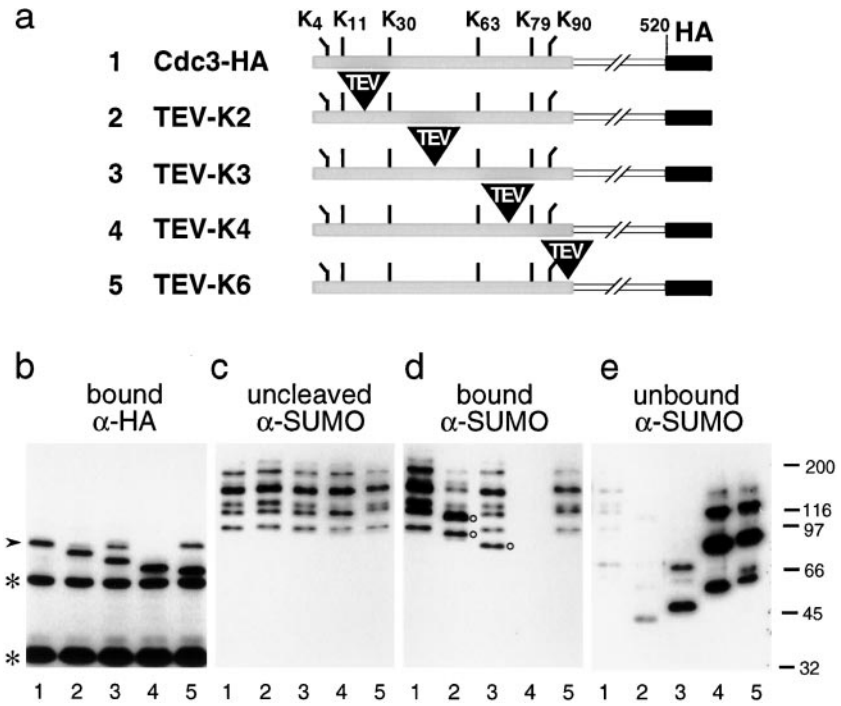

Figure 4. Single SUMO moieties are attached to multiple Lys residues in the NH_2-terminal domain of Cdc3. a, Diagram of TEV protease cleavage site-containing constructs, showing the six Lys residues in the NH_2-terminal domain of Cdc3 and the positions of introduced TEV cleavage sites. b–e, Exponential cultures of EJY300 (*cdc3*Δ) bearing plasmids expressing Cdc3-HA or one of the TEV site-containing Cdc3-HA constructs were arrested with nocodazole, lysed, and the lysates immunoprecipitated with an mAb against the HA epitope. Immunoprecipitated protein was treated with TEV protease while bound to the beads, and the resulting cleavage products were separated into an unbound fraction (e) and a bound fraction (b and d). The uncleaved proteins are shown in c. Fractions were analyzed by SDS-PAGE and immunoblotting with an mAb against the HA epitope (b) or a polyclonal antibody against SUMO (c–e). Lanes are numbered according to construct numbers in a. Asterisks indicate bands containing IgG. Arrow indicates uncleaved, unmodified Cdc3-HA. Open circles in d indicate the TEV cleavage products.

tation reduced the other mobility-altering factor without affecting SUMO conjugation. We do not know what this other factor is. It might be another posttranslational modification, but it is also possible that conjugates bearing the same number of SUMO moieties could have different mobilities resulting from SUMO attachment at different sites.

Mutational Analysis of Sumoylation Site Lys Residues on Septins

Inspection of the Cdc11 and Shs1 sequences for sumoylation site consensus sequences revealed that Cdc11 contained one such sequence near its COOH terminus and that Shs1 contained two such sequences in its COOH-terminal coiled-coil domain (Fig. 5 a). To determine the effects of eliminating these Lys residues on septin sumoylation and on cellular function, we made yeast strains in which the genomic copies of septins were replaced with mutant versions lacking these Lys residues. Deleting the coding sequence for the 94 NH_2-terminal residues of Cdc3 eliminated the vast majority of the SUMO-Cdc3 conjugates in nocodazole-arrested cells, confirming the conclusion that most SUMO is attached to this NH_2-terminal domain (Fig. 5 b, lanes 1 and 2). However, Cdc3-Δ94 was still sumoylated at a very low level by one copy of SUMO (Fig. 5 b, lane 2; note the band running at the position of full-length Cdc3-HA). This result was confirmed by immunoprecipitating with the anti-HA antibody and immunoblotting with an antibody against SUMO (data not shown). Mutating two more Lys residues in *CDC3*-Δ94, Lys-415 in the sequence IKQD, and Lys-443 in the sequence AKLE, had no effect on this residual sumoylation (data not shown). The only other sequence in Cdc3 that resembles the sumoylation site consensus sequence is the AKSD containing Lys-287, which is in the septin homology domain. This Lys residue is conserved in all members of the septin family in all organisms, except for Shs1 and one hypothetical open reading frame in *S. pombe*. Mutant *cdc3* containing a Lys to Arg mutation in this position was unable to complement the lethality of the *cdc3*Δ strain, even when all the NH_2-terminal sumoylation site Lys residues were present (data not shown). It is likely that this result reflects a requirement for this Lys residue in some septin function other than SUMO conjugation. When we mutated Lys-412 of Cdc11, and Lys-426 and Lys-437 of Shs1 to Arg, similar results were observed. In both cases, the vast majority of SUMO conjugates were eliminated, but a small amount of residual conjugation remained, reflecting low levels of SUMO conjugation at other sites (Fig 5 b, lanes 3–6; data not shown).

As all of the strains with sumoylation site mutations in only one of the septins still contained substantial SUMO rings at the bud neck, we proceeded to construct a triple mutant in which all of Cdc3, Cdc11, and Shs1 lacked the major sumoylation sites. Analysis of a series of strains in which progressively fewer septins contained sumoylation sites demonstrated that the majority of the total SUMO in nocodazole-arrested cells was attached to Cdc3 (Fig. 5 c, lane 2, cf lane 1) and that the most of the remainder was attached to Cdc11 or Shs1 (Fig. 5 c, lanes 2–4). Thus, septins are by far the most abundant SUMO conjugates at this point in the cell cycle. However, a longer exposure of this blot revealed a large number of lower abundance substrates in the triple mutant strain (data not shown).

To minimize any non-SUMO–related effects from deleting the entire Cdc3 NH_2-terminal domain, we constructed a different *cdc3* sumoylation site mutant in which all four attachment site Lys residues were replaced with Arg. This mutant's effects on Cdc3 sumoylation were indistinguishable from those of the deletion mutant (data not shown),

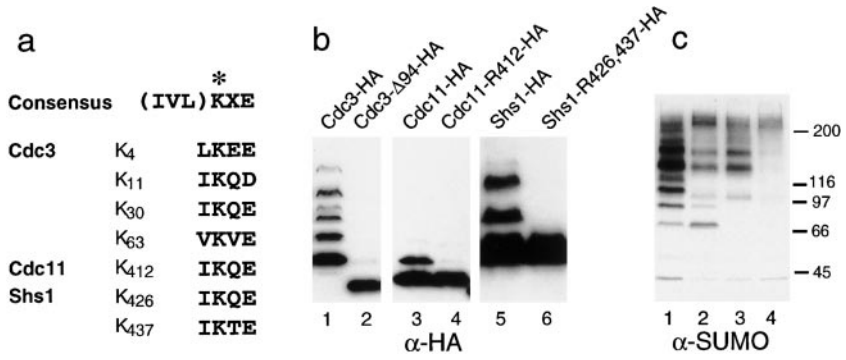

Figure 5. Mutational analysis of SUMO attachment site Lys residues in the septins. a, Sequences surrounding SUMO attachment sites in the septins. b and c, Whole cell lysates from nocodazole-arrested cultures were analyzed by SDS-PAGE and immunoblotting with an mAb against the HA epitope (b), or a polyclonal antibody against SUMO (c). b, Lane 1, EJY301; lane 2, EJY307; lane 3, EJY303; lane 4, EJY308; lane 5, EJY305; lane 6, EJY309. The HA-tagged septin in each strain is indicated over the lane. c, Lane 1, JD52 (wild-type); lane 2, EJY307 (*cdc3-Δ94-HA*); lane 3, EJY310 (*cdc3-Δ94-HA cdc11-R412-HA*), lane 4, EJY311 (*cdc3-Δ94-HA cdc11-R412-HA shs1-R426,437-HA*).

and subsequent experiments were done using this *cdc3* allele. We analyzed the sumoylation site triple mutant (*cdc3-R4,11,30,63 cdc11-R412 shs1-R426,437*) for phenotypes and found that in most respects it was very similar to the parental wild-type strain. Its growth rate was virtually indistinguishable from that of the wild-type (data not shown), with a doubling time of 95 min, versus 94 min for wild-type, a statistically insignificant difference. This strain was not hypersensitive to either high or low temperatures, to 1 M sorbitol, to DNA damaging agents (UV light or methyl methane sulfonate), to the microtubule depolymerizing drug benomyl, or to the cell wall perturbing agent Calcofluor white (data not shown). It mated efficiently and sporulated with the same efficiency as wild-type to produce viable segregants (data not shown). Haploid cells correctly positioned their bud sites axially, and most diploid cells positioned their bud sites bipolarly, although both this strain and the parental wild-type diploid strain had a significant frequency of cells with random bud sites (data not shown). The actin cytoskeleton, as visualized by rhodamine-phalloidin staining, also appeared normal in the triple mutant (data not shown).

We also analyzed the triple mutant by double-label immunofluorescence microscopy with antibodies against SUMO and against the HA tag on the septins. The triple mutant displayed a dramatic reduction in SUMO staining at the bud neck (Fig. 6, a–h), although a faint ring could be seen in a few cells (data not shown), and other cells contained a bulge of SUMO staining at the bud neck near the nuclear envelope that did not appear to colocalize completely with the mother cell half of the septin ring (Fig. 6 e). This slight SUMO localization to the bud neck probably

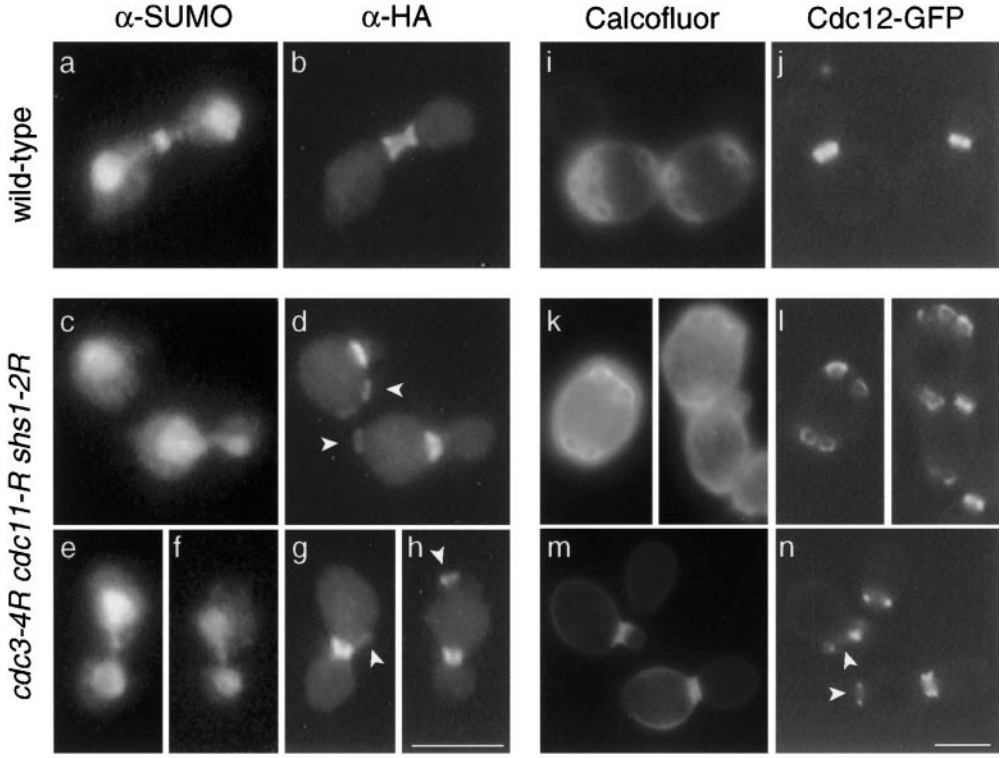

Figure 6. The triple sumoylation site septin mutant accumulates extra septin rings. a–h, EJY306 (*CDC3-HA*; a and b) or EJY318 (*cdc3-R4,11,30,63 cdc11-R412-HA shs1-R426,437-HA*; c–h) were analyzed by double-label immunofluorescence microscopy with a polyclonal antibody against SUMO (a, c, e, and f) and an mAb against the HA epitope (b, d, g, and h). i–n, Fluorescence microscopy of living log phase cells stained with Calcofluor, visualizing Calcofluor staining (i, k, and m) or Cdc12-GFP (j, l, and n). Strains used were EJY319 (*CDC12-GFP*; i and j) and EJY320 (*cdc3-R4,11,30,63 cdc11-R412-HA shs1-R426,437-HA CDC12-GFP*; k–n). Arrowheads indicate septin rings remaining from previous cell cycles. Bars, 5 μm.

resulted from the residual sumoylation of the septins, although some other bud neck protein may also be sumoylated at a very low level.

The striking difference that we noted between the triple mutant strain and wild-type was that in the mutant, at least one extra septin ring could be observed in virtually all budded cells (Fig. 6, d, g, and h). This is in contrast to the wild-type strain, in which budded cells never contained septin rings other than at the neck of the growing bud (Fig. 6 b). The presence of these extra septin rings was a synthetic phenotype of the triple mutant, as none of the single mutants or the *cdc11-R412 shs1-R426,437* double mutant had this property (data not shown). To test the hypothesis that the extra septin rings in the triple mutant were remnants of septin rings from previous cells divisions, we compared the localization of the extra septin rings with that of the bud scars. Every time an *S. cerevisiae* cell divides, the division site on the mother cell is marked by a chitin-containing bud scar, stainable with the fluorescent dye Calcofluor white, which persists through the lifetime of the cell. Although they sometimes had many bud scars, wild-type budded cells never contained more than the one septin ring at the base of the growing bud (Fig. 6, i and j). In the mutant, however, a septin ring colocalized with virtually every bud scar (Fig. 6, k and l), indicating that the extra septin rings are likely to be undisassembled septin rings from previous bud sites. Unlike mother cells, daughter cells do not have Calcofluor-staining structures marking the division site. Examination of budded cells lacking bud scars revealed that they always contained exactly one extra septin ring, indicating that daughter cells are also defective in septin ring disassembly (Fig. 6, m and n).

There are two simple reasons why the triple sumoylation site mutant might be defective in septin ring disassembly. One is that attachment of SUMO to the septin ring promotes disassembly. The other is that the sumoylation-site Lys residues also have some other function, and that this other function promotes septin ring disassembly. For example, the purpose of these Lys residues could be to serve as ubiquitination sites, or perhaps acetylation or methylation sites. One way to distinguish between these possibilities might be to determine whether mutants in the SUMO conjugation pathway also have septin ring disassembly defects. Examination of Cdc11 localization in *ubc9* (Fig. 7 a) and *uba2* (data not shown) ts mutants showed that no extra septin rings were visible in cells from either strain, either when grown at the permissive temperature or after transfer to the restrictive temperature. This result may suggest that SUMO conjugation, per se, does not promote septin ring disassembly. Alternatively, it may indicate that, although SUMO conjugation may promote septin ring disassembly, as long as these ts mutants retain enough SUMO conjugating activity to divide, they also retain sufficient SUMO conjugation to disassemble their septin rings.

In contrast to a previously published report (Takahashi et al., 1999), the levels of Cdc3 and Cdc11 did not decrease noticeably when the *ubc9* ts mutant was incubated at the nonpermissive temperature for 4 h (Fig. 7 b), and Cdc11 was still present at the bud neck in similar amounts as in wild-type (Fig. 7 a; data not shown). It is likely that the other septins were also present, as septins assemble cooperatively. However, the septin rings in arrested *ubc9* and *uba2* mutants were unlike those in wild-type preanaphase cells in that they appeared to be discontinuous in the middle (Fig. 7 a; data not shown), almost as in cells undergoing cytokinesis. This result may be a secondary effect of the prolonged G_2/M arrest, as we sometimes saw a similar effect in nocodazole-arrested cells, or, this observation may suggest that SUMO conjugation prevents septins from undergoing a reorganization usually associated with cytokinesis prematurely.

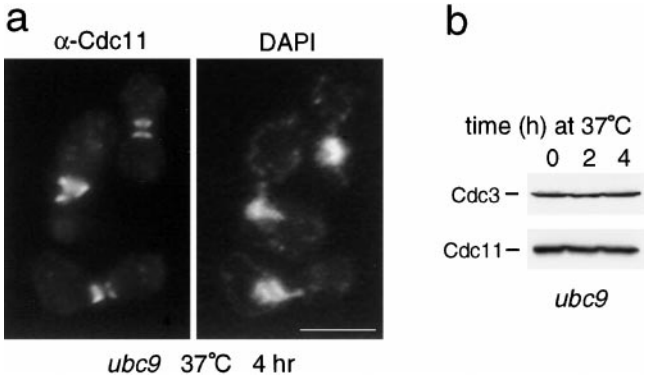

Figure 7. Septins are stable in a *ubc9* mutant. Strain YWO102 (*ubc9*) was grown to log phase in rich medium (YPD) at 25°C and shifted to 37°C for the indicated period of time. a, Cdc11 was visualized by immunofluorescence microscopy using a polyclonal antibody against Cdc11 and DNA by DAPI staining. Bar, 5 μm. b, Whole cell lysates were analyzed by SDS-PAGE and immunoblotting with a polyclonal antibody against Cdc3 (top) or against Cdc11 (bottom).

To test whether septins are ubiquitinated or degraded during cytokinesis, we synchronized a culture of *cdc15-2* cells by incubating them at 37°C, which arrests them in late anaphase, and releasing them at 25°C to allow them to complete cytokinesis (Fig. 8). Between 30 and 50 min after release, all the SUMO-conjugated forms of Cdc3 and Cdc11 disappeared from these cells. However, there was no significant reduction in the steady-state level of either Cdc3 or Cdc11 at this point, which is consistent with the observation by immunofluorescence microscopy that septin rings do not disappear suddenly at cytokinesis. Also, in several different experiments, we never observed high molecular weight ubiquitinated Cdc3 species. However, we did sometimes observe minor bands that might be degradation products of Cdc11 (Fig. 8 c) and of Cdc3-HA (data not shown). We conclude that, at most, a small fraction of Cdc3 and Cdc11 is degraded immediately at cytokinesis.

We also tested whether the sumoylation site triple mutant interacted genetically with either SUMO conjugation pathway mutants or septin mutants. A quadruple mutant also containing a chromosomally integrated version of the *uba2* ts10 allele grew at a range of rates similar to those seen with the *uba2* ts10 strain alone (data not shown), which grew very poorly and was heterogeneous. Thus, the attachment site mutations did not strongly exacerbate or suppress the phenotypes of the *uba2* ts10 mutant. However, when we crossed the sumoylation site triple mutant to a *cdc12-1* mutant, we obtained the surprising result that

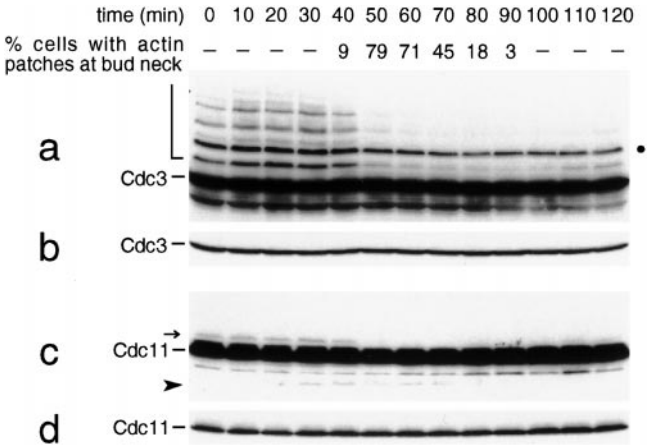

Figure 8. The steady-state levels of Cdc3 and Cdc11 do not fluctuate with the cell cycle. EJY321 (*cdc15-2*) was grown to exponential phase at 25°C in synthetic (SD–URA) medium, incubated at 37°C for 3 h, cooled briefly on ice, and returned to growth at 25°C. Samples taken at the indicated times after the culture was cooled were used to make whole cell lysates, which were analyzed by SDS-PAGE and immunoblotting with a polyclonal antibody against Cdc3 (a and b) or against Cdc11 (c and d). b and d are shorter exposures of a and c, respectively. Bands corresponding to unmodified Cdc3 and Cdc11 are indicated. A half-open square bracket designates high molecular weight SUMO-Cdc3 conjugates. A circle indicates a band that cross-reacts with the anti-Cdc3 antibody. A SUMO-Cdc11 conjugate is indicated with an arrow, and a possible proteolytic breakdown product of Cdc11 with an arrowhead. The percentage of cells in which the actin patches are polarized toward the bud neck, an indication of cells undergoing cytokinesis, is listed over the lanes. A dash indicates <1%.

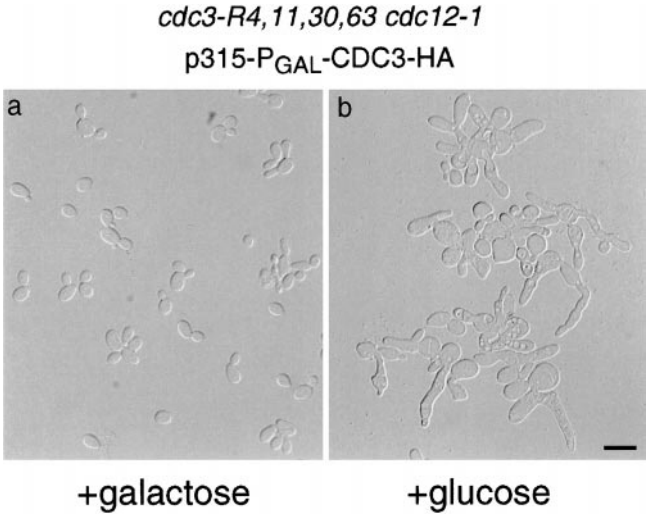

Figure 9. The *cdc3* attachment site mutant is synthetically lethal with *cdc12-1*. EJY323 (*cdc3-R4,11,30,63 cdc12-1*) carrying p315-P_{GAL}-CDC3-HA was grown to exponential phase at 25°C in YPG (a); or YPG-grown cells were isolated, resuspended in YPD, and then incubated at 25°C for 24 h (b). Bar, 10 μm.

the *cdc3-R4,11,30,63* mutation alone was synthetically lethal with the *cdc12-1* mutation. *cdc12-1* single mutants grow well with near normal morphology at 25°C, but lose septin rings and develop the distinctive phenotypes of septin mutants at 37°C (see introduction). At 25°C, *cdc3-R4,11,30,63 cdc12-1* cells overexpressing wild-type *CDC3-HA* exhibited near normal morphology (Fig. 9 a). When *CDC3-HA* expression was repressed, the double mutant developed the phenotypes of septin mutants, even at 25°C, producing branched, elongated cells and failing to undergo cytokinesis (Fig. 9 b). This effect was not general for all septin mutants, as the sumoylation site mutations did not exacerbate the phenotypes of the *cdc10-1* mutant (data not shown).

Discussion

We have identified the septins Cdc3, Cdc11, and Shs1 as the three SUMO conjugation pathway substrates that account for the most abundant sumoylated species during yeast mitosis. Septin sumoylation was highly regulated, occurring only during mitosis and only on the mother cell side of the bud neck. We identified the major SUMO attachment site Lys residues in these septins and found that they are surrounded by a short consensus sequence that has also been observed around the mammalian SUMO attachment sites (Desterro et al., 1998; Kamitani et al., 1998a; Mahajan et al., 1998; Matunis et al., 1998; Duprez et al., 1999; Sternsdorf et al., 1999). Multiple copies of SUMO could be linked to a single Cdc3 polypeptide by attachment of single SUMO moieties to several different Lys residues. We could see no evidence of SUMO chain formation analogous to the chains formed by Ub. A mutant lacking these sumoylation sites on septins grew well and was not hypersensitive to the stress conditions tested, but was deficient in disassembly of the septin rings after cytokinesis. The *cdc3* sumoylation site mutation also showed synthetic lethality with the *cdc12-1* mutation. These results raise many interesting issues regarding the regulation of SUMO conjugation and the structural and functional alterations of the septin ring that take place during and after cytokinesis.

While this manuscript was in preparation, another paper was published reporting that Cdc3 is a SUMO substrate (Takahashi et al., 1999), but there are many contradictions between the two reports. For example, they fail to find that Cdc11 is modified and they observe that SUMO is found primarily as the unconjugated form, with small amounts of low molecular weight conjugates, rather than primarily in high molecular weight conjugates, as observed by others (Johnson et al., 1997; Li and Hochstrasser, 1999). These results can be explained by noting that their protocol for preparing yeast lysates does not, in our experience, inhibit the isopeptidases that cleave SUMO off its substrates virtually instantly when cells are lysed under native conditions. Other groups working in this field lyse cells under denaturing conditions to prevent this problem (Johnson et al., 1997; Desterro et al., 1998; Kamitani et al., 1998b). Despite this problem, Takahashi et al. (1999) do detect a SUMO conjugate of a Cdc3-GFP fusion protein. Using this reporter, they make the following observations that contradict our results: that there is only a single SUMO-Cdc3-GFP conjugate band; that 50–100% of the

total Cdc3-GFP is sumoylated (we estimate that, at most, 5% of Cdc3 or Cdc3-HA was sumoylated; Figs. 1, 2, 5, and 8); that Cdc3-GFP is sumoylated at this same high level in α-factor-, hydroxyurea- and nocodazole-arrested cells; that the SUMO-Cdc3-GFP conjugate persists through cell lysis under native conditions (in our hands, Cdc3-HA is rapidly desumoylated under these conditions; data not shown); and that Cdc3-GFP disappears from the bud neck upon transfer of *ubc9* ts cells to the nonpermissive temperature. The first four of these results also contradict other published reports about Cdc3, where Cdc3 runs on SDS-PAGE as a single band of the expected size for the unmodified protein (Kim et al., 1991; Frazier et al., 1998). It is likely that the Cdc3-GFP reporter protein is responsible for these discrepancies. There is no evidence to support the statement that this protein is functional, and all of these experiments have been performed in strains also containing the wild-type untagged genomic copy of *CDC3*. The findings that the protein level of Cdc3-GFP decreases during cytokinesis and in *ubc9* ts cells at the nonpermissive temperature contradict our results and appear to involve technical problems with their Western blots. The most interesting discrepancy is that they observe SUMO localizing to both sides of the bud neck, whereas we see it only on the mother cell side. This observation could result from a strain difference, but it seems more likely that their result is a phenotype of HA-SUMO overexpression.

Our results indicate that the G_2/M cell cycle arrest phenotypes of the SUMO conjugation pathway mutants probably do not result from a reduction in septin sumoylation. The sumoylation site triple mutant, which eliminated the vast majority of SUMO conjugation to the septins, grew at the same rate as wild-type and did not exhibit any cell cycle arrest phenotype. Furthermore, a *uba2* ts mutation did not exacerbate the phenotype of the triple mutant, indicating that SUMO conjugation to other sites on the septins or to some other substrate is not compensating for the loss of the major septin sumoylation sites. It is still possible that the minor septin sumoylation sites play a distinct essential role for which the major sites cannot substitute. However, we believe it is more likely that the SUMO substrates involved in the essential and cell cycle-related roles of the SUMO pathway participate in an entirely different cellular function, possibly chromosome segregation, as *SMT3*, the SUMO-encoding gene, was identified as a high copy suppressor of a mutant impaired in chromosome segregation (Meluh and Koshland, 1995).

Septin sumoylation might be controlled by the cell cycle machinery through regulation of SUMO attachment, SUMO removal, or both. It is difficult to determine the fate of sumoylated septins at cytokinesis because of the small fraction modified, but it is most likely that the septins are desumoylated by a SUMO-specific isopeptidase such as Ulp1 or the similar protein Ulp2/Smt4 (Li and Hochstrasser, 1999). In fact, one possibility is that the level of SUMO–septin conjugates at all stages in the cell cycle reflects a dynamic equilibrium between sumoylation and desumoylation. We found that SUMO–septin conjugates disappeared rapidly from nocodazole-arrested *ubc9* ts cells, but not from wild-type cells, upon shift to the nonpermissive temperature (data not shown), suggesting that SUMO may have to be continually reattached to maintain a constant level of septin sumoylation. Thus, septins may be constitutively desumoylated, which would allow the level of SUMO conjugates to be tightly regulated solely by controlling the rate of the conjugation reaction.

Several issues depend on the structure of the septin-containing neck ring, which has not been described in detail. Purified septins form linear filaments in vitro, and the present model for the structure of the ring holds that it consists of parallel septin filaments running through the bud neck parallel to the mother-bud axis (Field et al., 1996; Frazier et al., 1998). These filaments are linked laterally to form the ring by an unknown mechanism involving the Nim1-related kinases Gin4, Hsl1, and Kcc4 (Longtine et al., 1998; Barral et al., 1999). Other proteins associate with the septin ring in four distinct arrangements: throughout the septin ring, on the mother cell side, on the bud side, and in the middle between the mother cell and bud. One model for how such regions might be established derives from the fact that the mother and bud sides of the neck ring are assembled at different points in the cell cycle (DeMarini et al., 1997). Thus, different septin-associated proteins could be incorporated into the different sides, establishing stable zones within the ring. Other proteins, such as SUMO conjugation pathway enzymes, could specifically bind the asymmetrically localized proteins initially incorporated into the different regions. A second model relies on the potential inherent polarity of the septin filaments running through the bud neck. Associated proteins might move along the filaments in one direction or the other until they reach the mother or bud side of the ring.

The data on septin-SUMO conjugation is less consistent with the model where various regions are preestablished, because it is possible for the daughter side to be sumoylated. Takahashi et al. (1999) observed SUMO on both sides of the bud neck, probably as a result of HA-SUMO overexpression, and we also observed SUMO on both sides of some septin rings in nocodazole-arrested cultures (data not shown). Thus, septin sumoylation appears to be dosage dependent, such that the mother cell side is modified first, with the daughter cell side modified when the system is overexpressed or abnormally induced.

Another question is why such a small fraction of each of the septins is modified. If the septin polypeptides that are sumoylated are functionally and structurally equivalent to the ones that are not, it would be less likely that SUMO is blocking Lys residues against attachment of some other modification, since these Lys residues would still be available on the vast majority of potential substrates. However, the various septin polypeptides may not be equivalent, either because all positions in the septin lattice may not be equivalent structurally or because of the presence of other posttranslational modifications. We did see variant forms of SUMO-Cdc3 conjugates, which may bear another posttranslational modification. There did not appear to be proportional amounts of a corresponding variant of unsumoylated Cdc3, suggesting that the other modification may target the same subpopulation or that one modification is a prerequisite for the other.

The triple sumoylation site mutant is the first mutant isolated with a defect in septin ring disassembly. We have mentioned two models for how the triple mutant might affect disassembly of the septin ring. One is that SUMO it-

self promotes septin ring disassembly, and the other is that the sumoylation-site Lys residues play some other role in disassembly, possibly by serving as ubiquitination sites. In the second model, SUMO might play a regulatory role by preventing the Lys residues from taking part in the other function. Alternatively, the other function might be completely independent from SUMO.

Any model for SUMO involvement in septin ring disassembly has to explain two sets of seemingly contradictory results. One is that SUMO is attached only to the mother cell side of the bud neck, but the septin rings fail to be disassembled in both the mother cell and in the daughter cell (Fig. 6). The other is that SUMO–septin conjugates disappear suddenly at cytokinesis, but disassembly of the septin rings does not take place until G_1 of the next cycle. The simplest way to explain the symmetry of the phenotype is if the SUMO-related event takes place in the center of the septin ring. During cytokinesis, an actomyosin contractile ring forms in the center of the septin ring (Bi et al., 1998; Lippincott and Li, 1998b) and colocalizes with other proteins required for contractile ring function (Epp and Chant, 1997; Kamei et al., 1998; Lippincott and Li, 1998a,b). Contraction of the ring is triggered by an unknown mechanism close to the same time the SUMO ring disappears. A SUMO–septin-related event could take place in this same region that would be required for the complete disassembly of both the mother and daughter cell sides of the ring. It is worth noting that the old septin rings in the sumoylation site mutant contained much less septin than the ring at the base of a growing bud, indicating that some disassembly did take place. Perhaps the remaining structure is "capped" in such a way that a post-translational modification at the SUMO attachment sites is required to remove it.

Either model can also explain the timing of SUMO removal and septin ring disassembly. If SUMO itself promotes disassembly, SUMO might be involved in an initial event, either the SUMO-dependent association with the septin ring of another protein that is later involved in disassembly, or direct SUMO participation in a preliminary disassembly event, whose effects only become apparent later in the cell cycle. Using this model, it is easier to explain the fact that only a small fraction of each of the septins is modified, because a small amount of modified septin might be sufficient to attract some other protein to the bud neck. On the other hand, the model where SUMO prevents disassembly by inhibiting some other process is more consistent with the timing of desumoylation, as septin ring disassembly actually starts after SUMO is removed. Removal of SUMO might serve as an initiation signal, allowing access to other proteins that trigger the septin rearrangements that take place during and after cytokinesis. However, as mentioned above, the main problem with this model is the extremely low percentage of septin polypeptides that are actually modified. This seems like an inefficient way to block an interaction or modification, since >95% of all sites still would be available. Another key question related to this model is whether any fraction of the septins is ubiquitinated and degraded at this point in the cell cycle. We were unable to detect high molecular weight Ub conjugates or any dramatic reductions in the steady-state levels of Cdc3 or Cdc11, but it is possible that a small fraction of the septins may be degraded during cytokinesis.

Another important question is whether septin sumoylation plays other roles in initiation of anaphase, during anaphase, or in cytokinesis. It is still possible that septin sumoylation participates in a process carried out by two or more partially redundant pathways, or that it is part of a checkpoint monitoring a process that we have not perturbed in any of our experiments. Further analysis of genes that interact with the septin sumoylation site mutant should lead to a clearer picture of the role of septin sumoylation in yeast growth.

We thank John Pringle, Mark Longtine, Maria Yuste, Fred Cross, Mike Rout, Jonathan Rosenblum, Jürgen Dohmen, and Stefan Jentsch for strains, plasmids, and antibodies; and members of the Rockefeller University Protein/DNA Technology Center for DNA sequencing and especially Farzin Gharahdaghi for MALDI-TOF analysis. We also thank John Pringle and Ray Deshaies for helpful discussions, and Lucy Pemberton, Markus Albertini, and especially, Nabeel Yaseen and Jonathan Rosenblum, for critical reading of the manuscript.

This work was supported by the Howard Hughes Medical Institute (G. Blobel).

Submitted: 15 September 1999
Revised: 11 October 1999
Accepted: 20 October 1999

References

Ausubel, F.M., R. Brent, R.E. Kingston, D.D. Moore, J.A. Smith, J.G. Seidman, and K. Struhl. 1994. Current Protocols in Molecular Biology. Wiley-Interscience, New York.

Barral, Y., M. Parra, S. Bidlingmaier, and M. Snyder. 1999. Nim1-related kinases coordinate cell cycle progression with the organization of the peripheral cytoskeleton in yeast. *Genes Dev*. 13:176–187.

Bi, E., P. Maddox, D.J. Lew, E.D. Salmon, J.N. McMillan, E. Yeh, and J.R. Pringle. 1998. Involvement of an actomyosin contractile ring in *Saccharomyces cerevisiae* cytokinesis. *J. Cell Biol*. 142:1301–1312.

Boeke, J.D., F. LaCroute, and G.R. Fink. 1984. A positive selection for mutants lacking orotidine-5′-phosphate decarboxylase activity in yeast: 5-fluoro-orotic acid resistance. *Mol. Gen. Genet*. 197:345–346.

Carroll, C.W., R. Altman, D. Schieltz, J.R. Yates, and D. Kellogg. 1998. The septins are required for the mitosis-specific activation of the Gin4 kinase. *J. Cell Biol*. 143:709–717.

Chant, J., M. Mischke, E. Mitchell, I. Herskowitz, and J.R. Pringle. 1995. Role of Bud3p in producing the axial budding pattern of yeast. *J. Cell Biol*. 129: 767–778.

DeMarini, D.J., A.E. Adams, H. Fares, C. De Virgilio, G. Valle, J.S. Chuang, and J.R. Pringle. 1997. A septin-based hierarchy of proteins required for localized deposition of chitin in the *Saccharomyces cerevisiae* cell wall. *J. Cell Biol*. 139:75–93.

Desterro, J.M., J. Thomson, and R.T. Hay. 1997. Ubch9 conjugates SUMO but not ubiquitin. *FEBS Lett*. 417:297–300.

Desterro, J.M., M.S. Rodriguez, and R.T. Hay. 1998. SUMO-1 modification of IκBα inhibits NF-κB activation. *Mol. Cell*. 2:233–239.

Dohmen, R.J., R. Stappen, J.P. McGrath, H. Forrova, J. Kolarov, A. Goffeau, and A. Varshavsky. 1995. An essential yeast gene encoding a homolog of ubiquitin-activating enzyme. *J. Biol. Chem*. 270:18099–18109.

Duprez, E., A.J. Saurin, J.M. Desterro, V. Lallemand-Breitenbach, K. Howe, M.N. Boddy, E. Solomon, H. de The, R.T. Hay, and P.S. Freemont. 1999. SUMO-1 modification of the acute promyelocytic leukaemia protein PML: implications for nuclear localisation. *J. Cell Sci*. 112:381–393.

Epp, J.A., and J. Chant. 1997. An IQGAP-related protein controls actin-ring formation and cytokinesis in yeast. *Curr. Biol*. 7:921–929.

Field, C.M., O. al-Awar, J. Rosenblatt, M.L. Wong, B. Alberts, and T.J. Mitchison. 1996. A purified *Drosophila* septin complex forms filaments and exhibits GTPase activity. *J. Cell Biol*. 133:605–616.

Field, J., J. Nikawa, D. Broek, B. MacDonald, L. Rodgers, I.A. Wilson, R.A. Lerner, and M. Wigler. 1988. Purification of a RAS-responsive adenylyl cyclase complex from *Saccharomyces cerevisiae* by use of an epitope addition method. *Mol. Cell. Biol*. 8:2159–2165.

Finley, D., E. Özkaynak, and A. Varshavsky. 1987. The yeast polyubiquitin gene is essential for resistance to high temperatures, starvation, and other stresses. *Cell*. 48:1035–1046.

Frazier, J.A., M.L. Wong, M.S. Longtine, J.R. Pringle, M. Mann, T.J. Mitchison, and C. Field. 1998. Polymerization of purified yeast septins: evidence

that organized filament arrays may not be required for septin function. *J. Cell Biol*. 143:737–749.

Gharahdaghi, F., M. Kirchner, J. Fernandez, and S.M. Mische. 1996. Peptide-mass profiles of polyvinylidene difluoride-bound proteins by matrix-assisted laser desorption/ionization time-of-flight mass spectrometry in the presence of nonionic detergents. *Anal. Biochem*. 233:94–99.

Giot, L., and J.B. Konopka. 1997. Functional analysis of the interaction between Afr1p and the Cdc12p septin, two proteins involved in pheromone-induced morphogenesis. *Mol. Biol. Cell*. 8:987–998.

Gong, L., T. Kamitani, K. Fujise, L.S. Caskey, and E.T. Yeh. 1997. Preferential interaction of sentrin with a ubiquitin-conjugating enzyme, Ubc9. *J. Biol. Chem*. 272:28198–28201.

Harlow, E., and D. Lane. 1988. Antibodies: A Laboratory Manual. Cold Spring Harbor Laboratory Press, Cold Spring Harbor, NY.

Hershko, A., and A. Ciechanover. 1998. The ubiquitin system. *Annu. Rev. Biochem*. 67:425–479.

Johnson, E.S., and G. Blobel. 1997. Ubc9p is the conjugating enzyme for the ubiquitin-like protein Smt3p. *J. Biol. Chem*. 272:26799–26802.

Johnson, E.S., B. Bartel, W. Seufert, and A. Varshavsky. 1992. Ubiquitin as a degradation signal. *EMBO (Eur. Mol. Biol. Org.) J*. 11:497–505.

Johnson, E.S., I. Schwienhorst, R.J. Dohmen, and G. Blobel. 1997. The ubiquitin-like protein Smt3p is activated for conjugation to other proteins by an Aos1p/Uba2p heterodimer. *EMBO (Eur. Mol. Biol. Org.) J*. 16:5509–5519.

Kamei, T., K. Tanaka, T. Hihara, M. Umikawa, H. Imamura, M. Kikyo, K. Ozaki, and Y. Takai. 1998. Interaction of Bnr1p with a novel Src homology 3 domain-containing Hof1p. Implication in cytokinesis in *Saccharomyces cerevisiae*. *J. Biol. Chem*. 273:28341–28345.

Kamitani, T., K. Kito, H.P. Nguyen, H. Wada, T. Fukuda-Kamitani, and E.T. Yeh. 1998a. Identification of three major sentrinization sites in PML. *J. Biol. Chem*. 273:26675–26682.

Kamitani, T., H.P. Nguyen, K. Kito, T. Fukuda-Kamitani, and E.T. Yeh. 1998b. Covalent modification of PML by the sentrin family of ubiquitin-like proteins. *J. Biol. Chem*. 273:3117–3120.

Kim, H.B., B.K. Haarer, and J.R. Pringle. 1991. Cellular morphogenesis in the *Saccharomyces cerevisiae* cell cycle: localization of the CDC3 gene product and the timing of events at the budding site. *J. Cell Biol*. 112:535–544.

Li, S.J., and M. Hochstrasser. 1999. A new protease required for cell-cycle progression in yeast. *Nature*. 398:246–251.

Lippincott, J., and R. Li. 1998a. Dual function of Cyk2, a cdc15/PSTPIP family protein, in regulating actomyosin ring dynamics and septin distribution. *J. Cell Biol*. 143:1947–1960.

Lippincott, J., and R. Li. 1998b. Sequential assembly of myosin II, an IQGAP-like protein, and filamentous actin to a ring structure involved in budding yeast cytokinesis. *J. Cell Biol*. 140:355–366.

Longtine, M.S., D.J. DeMarini, M.L. Valencik, O.S. Al-Awar, H. Fares, C. De Virgilio, and J.R. Pringle. 1996. The septins: roles in cytokinesis and other processes. *Curr. Opin. Cell Biol*. 8:106–119.

Longtine, M.S., H. Fares, and J.R. Pringle. 1998. Role of the yeast Gin4p protein kinase in septin assembly and the relationship between septin assembly and septin function. *J. Cell Biol*. 143:719–736.

Mahajan, R., C. Delphin, T. Guan, L. Gerace, and F. Melchior. 1997. A small ubiquitin-related polypeptide involved in targeting RanGAP1 to nuclear pore complex protein RanBP2. *Cell*. 88:97–107.

Mahajan, R., L. Gerace, and F. Melchior. 1998. Molecular characterization of the SUMO-1 modification of RanGAP1 and its role in nuclear envelope association. *J. Cell Biol*. 140:259–270.

Matunis, M.J., E. Coutavas, and G. Blobel. 1996. A novel ubiquitin-like modification modulates the partitioning of the Ran-GTPase-activating protein RanGAP1 between the cytosol and the nuclear pore complex. *J. Cell Biol*. 135:1457–1470.

Matunis, M.J., J. Wu, and G. Blobel. 1998. SUMO-1 modification and its role in targeting the Ran GTPase-activating protein, RanGAP1, to the nuclear pore complex. *J. Cell Biol*. 140:499–509.

Meluh, P.B., and D. Koshland. 1995. Evidence that the MIF2 gene of *Saccharomyces cerevisiae* encodes a centromere protein with homology to the mammalian centromere protein CENP-C. *Mol. Biol. Cell*. 6:793–807.

Mino, A., K. Tanaka, T. Kamei, M. Umikawa, T. Fujiwara, and Y. Takai. 1998. Shs1p: a novel member of septin that interacts with spa2p, involved in polarized growth in *Saccharomyces cerevisiae*. *Biochem. Biophys. Res. Commun*. 251:732–736.

Müller, S., M.J. Matunis, and A. Dejean. 1998. Conjugation with the ubiquitin-related modifier SUMO-1 regulates the partitioning of PML within the nucleus. *EMBO (Eur. Mol. Biol. Org.) J*. 17:61–70.

Okuma, T., R. Honda, G. Ichikawa, N. Tsumagari, and H. Yasuda. 1999. In vitro SUMO-1 modification requires two enzymatic steps, E1 and E2. *Biochem. Biophys. Res. Commun*. 254:693–698.

Okura, T., L. Gong, T. Kamitani, T. Wada, I. Okura, C.F. Wei, H.M. Chang, and E.T. Yeh. 1996. Protection against Fas/APO-1- and tumor necrosis factor-mediated cell death by a novel protein, sentrin. *J. Immunol*. 157:4277–4281.

Pringle, J.R. 1991. Staining of bud scars and other cell wall chitin with calcofluor. *In* Guide to Yeast Genetics and Molecular Biology. Vol. 194. C. Guthrie and G.R. Fink, editors. Academic Press, San Diego, CA. 732–735.

Pringle, J.R., A.E.M. Adams, D.G. Drubin, and B.K. Haarer. 1991. Immunofluorescence methods for yeast. *In* Guide to Yeast Genetics and Molecular Biology. Vol. 194. C. Guthrie and G.R. Fink, editors. Academic Press, San Diego, CA. 565–602.

Rosenblum, J.S., L.F. Pemberton, N. Bonifaci, and G. Blobel. 1998. Nuclear import and the evolution of a multifunctional RNA-binding protein. *J. Cell Biol*. 143:887–899.

Saitoh, H., D.B. Sparrow, T. Shiomi, R.T. Pu, T. Nishimoto, T.J. Mohun, and M. Dasso. 1998. Ubc9p and the conjugation of SUMO-1 to RanGAP1 and RanBP2. *Curr. Biol*. 8:121–124.

Sanders, S.L., and I. Herskowitz. 1996. The BUD4 protein of yeast, required for axial budding, is localized to the mother/BUD neck in a cell cycle-dependent manner. *J. Cell Biol*. 134:413–427.

Schwarz, S.E., K. Matuschewski, D. Liakopoulos, M. Scheffner, and S. Jentsch. 1998. The ubiquitin-like proteins SMT3 and SUMO-1 are conjugated by the UBC9 E2 enzyme. *Proc. Natl. Acad. Sci. USA*. 95:560–564.

Seufert, W., B. Futcher, and S. Jentsch. 1995. Role of a ubiquitin-conjugating enzyme in degradation of S- and M-phase cyclins. *Nature*. 373:78–81.

Shen, Z., P.E. Pardington-Purtymun, J.C. Comeaux, R.K. Moyzis, and D.J. Chen. 1996. Associations of UBE2I with RAD52, UBL1, p53, and RAD51 proteins in a yeast two-hybrid system. *Genomics*. 37:183–186.

Sherman, F., G.R. Fink, and J.B. Hicks. 1986. Methods in Yeast Genetics. Cold Spring Harbor Laboratory Press, Cold Spring Harbor, NY.

Sikorski, R.S., and P. Hieter. 1989. A system of shuttle vectors and yeast host strains designed for efficient manipulation of DNA in *Saccharomyces cerevisiae*. *Genetics*. 122:19–27.

Sternsdorf, T., K. Jensen, B. Reich, and H. Will. 1999. The nuclear dot protein sp100, characterization of domains necessary for dimerization, subcellular localization, and modification by small ubiquitin-like modifiers. *J. Biol Chem*. 274:12555–12566.

Sternsdorf, T., K. Jensen, and H. Will. 1997. Evidence for covalent modification of the nuclear dot-associated proteins PML and sp100 by PIC1/SUMO-1. *J. Cell Biol*. 139:1621–1634.

Takahashi, Y., M. Iwase, M. Konishi, M. Tanaka, A. Toh-e, and Y. Kikuchi. 1999. Smt3, a SUMO-1 homolog, is conjugated to Cdc3, a component of septin rings at the mother-bud neck in budding yeast. *Biochem. Biophys. Res. Commun*. 259:582–587.

Yaffe, M.P., and G. Schatz. 1984. Two nuclear mutations that block mitochondrial protein import in yeast. *Proc. Natl. Acad. Sci. USA*. 81:4819–4823.